

Resolved photoproduction of the B_c meson in electron-proton collisions

Na Cai,^{a,b,c} Xi-Jie Zhan,^{a,b,c,1} Tai-Fu Feng^{a,b,c}

^a*Department of Physics, Hebei University, Baoding 071002, China*

^b*Hebei Key Laboratory of High-precision Computation and Application of Quantum Field Theory, Baoding 071002, China*

^c*Hebei Research Center of the Basic Discipline for Computational Physics, Baoding 071002, China*

ABSTRACT: We present a systematic study of B_c meson photoproduction at electron–proton colliders within the framework of nonrelativistic QCD (NRQCD) factorization. In addition to the dominant direct channel $\gamma + g \rightarrow B_c + X$, we include resolved contributions initiated by $g + g$ and $q + \bar{q}$ ($q = u, d, s$) subprocesses. Total cross sections and transverse-momentum distributions are calculated for several collider configurations, including HERA, LHeC, FCC-*ep*, and EIC. The numerical results show that the $\gamma + g$ channel provides the leading contribution to the total cross section, while the resolved $g + g$ channel yields a non-negligible correction at the level of $\mathcal{O}(10\%)$ in the low- p_T region where most events are produced. The $q + \bar{q}$ channel is found to be numerically insignificant.

¹Corresponding author.

Contents

1	Introduction	1
2	Formulation and calculation	2
3	Numerical results and discussions	3
4	Summary	7

1 Introduction

The B_c meson is a distinctive heavy-flavored hadron in the Standard Model, consisting of a bottom quark and a charm antiquark (or charge-conjugated state). As the only known meson composed of two heavy quarks of different flavors, the B_c system occupies a unique position between charmonium and bottomonium. Its spectroscopy, decay properties, and production mechanisms provide an important testing ground for heavy-quark dynamics, nonrelativistic effective theories, and nonperturbative aspects of Quantum Chromodynamics (QCD).

At high-energy colliders, the production of B_c mesons is governed predominantly by strong interactions. In contrast to quarkonium production, the formation of a B_c meson requires the simultaneous production of both a $b\bar{b}$ and a $c\bar{c}$ pair within a single hard scattering. Consequently, its production rate is suppressed relative to conventional heavy quarkonia, while remaining fully calculable within perturbative QCD. The hard subprocesses involve energy scales set by the heavy-quark masses, where perturbation theory is applicable, whereas the subsequent hadronization into a bound $b\bar{c}$ state probes the transition to the nonperturbative regime. This interplay makes B_c production a sensitive probe of QCD factorization and heavy-quark binding dynamics [1, 2].

Experimentally, the existence of the B_c meson was first firmly established by the CDF Collaboration in 1998 through analyses of proton–antiproton collision data at the Tevatron [3, 4]. In 2014, the ATLAS Collaboration reported the observation of the radially excited $B_c(2S)$ states [5]. These results were subsequently confirmed and refined by the CMS and LHCb Collaborations in 2019 with higher statistical significance and improved mass resolution [6, 7]. More recently, further experimental advances have led to the observation of orbitally excited B_c states [8]. To date, all observations of B_c mesons and their excited states have been obtained exclusively at hadron colliders.

Theoretical investigations of B_c meson production have been pursued across a wide range of collision environments and mechanisms. At hadron colliders such as the Tevatron and the LHC, dominant production channels arise from gluon–gluon fusion and heavy-quark fragmentation, calculable within the nonrelativistic QCD (NRQCD) factorization

framework at leading and higher orders in α_s [1, 2, 9–27]. Beyond hadronic collisions, B_c production has also been studied in the context of high-luminosity electron–positron colliders [28–39]. Indirect sources of B_c mesons through decays of heavy particles have been explored [40–49], such as the top quark, W boson and Higgs boson, highlighting the role of heavy-particle decay as a complementary production channel at high energies. An important class of processes at e^+e^- or electron–proton machines involves photoproduction, where initial-state radiation or Weizsäcker–Williams photons interact to produce a B_c meson accompanied by heavy quarks [32, 48, 50–53]. Detailed studies at e^+e^- colliders show that both direct $\gamma\gamma \rightarrow B_c + b + \bar{c}$ and resolved photon channels can yield substantial production rates under suitable collider configurations [54]. Previous studies of B_c photoproduction have mostly focused on the direct $\gamma + g$ channel, while the role of resolved photon contributions has received less attention, especially in the kinematic regime relevant for future high-luminosity ep colliders. In this work, based on the framework of non-relativistic QCD (NRQCD) [55], we proceed to investigate the photoproduction of B_c mesons at electron–proton colliders, with particular emphasis on including resolved processes.

2 Formulation and calculation

Within the framework of the Weizsäcker–Williams approximation (WWA), the energy distribution of photons originating from bremsstrahlung emission can be expressed as [56]

$$f_{\gamma/e}(x) = \frac{\alpha}{2\pi} \left[\frac{1 + (1-x)^2}{x} \log \frac{Q_{\max}^2}{Q_{\min}^2} + 2m_e^2 x \left(\frac{1}{Q_{\max}^2} - \frac{1}{Q_{\min}^2} \right) \right], \quad (2.1)$$

where $x = E_\gamma/E_e$ denotes the fraction of the longitudinal momentum carried by the emitted photon, α is the electromagnetic fine-structure constant, and the kinematic limits are given by $Q_{\min}^2 = m_e^2 x^2 / (1-x)$ and $Q_{\max}^2 = (E_e \theta_e)^2 (1-x) + Q_{\min}^2$. The parameter $\theta_e = 32$ mrad corresponds to the maximum allowed scattering angle of the outgoing electron, imposed to ensure that the emitted photon remains quasi-real.

Within the NRQCD factorization formalism, the cross section for B_c photoproduction at an electron–proton collider can be written in a factorized form as

$$\begin{aligned} & d\sigma(e^- + P \rightarrow B_c + X) \\ &= \int dx_1 dx_2 f_{\gamma/e}(x_1) \sum_j f_{j/P}(x_2) \sum_i \int dx_i f_{i/\gamma}(x_i) \\ & \times \sum_n d\hat{\sigma}(ij \rightarrow c\bar{b}[n] + b + \bar{c}) \langle \mathcal{O}^{B_c}[n] \rangle. \end{aligned} \quad (2.2)$$

Here $f_{j/P}$ denotes the parton distribution function (PDF) of parton j inside the proton, while $f_{i/\gamma}$ ($i = \gamma, g, u, d, s$) represents the Glück–Reya–Schienbein (GRS) distribution function of parton i in the photon [57]. The special case $f_{\gamma/\gamma}(x) = \delta(1-x)$ corresponds to the direct photoproduction contribution. The resolved photoproduction channels effectively

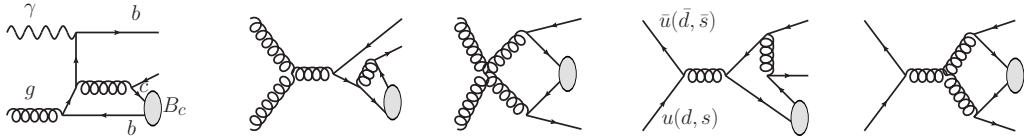


Figure 1. Some typical Feynman diagrams for calculating the partonic cross section $\hat{\sigma}$ of B_c photoproduction at ep collider. The diagrams are drawn by JaxoDraw [60].

colliders	\sqrt{S}	E_e	E_P
HERA	319 GeV	27.5 GeV	920 GeV
LHeC-1	1.30 TeV	60 GeV	7 TeV
LHeC-2	1.98 TeV	140 GeV	7 TeV
FCC- <i>ep</i> -1	7.07 TeV	250 GeV	50 TeV
FCC- <i>ep</i> -2	10.0 TeV	500 GeV	50 TeV
EIC-1	45 GeV	5 GeV	100 GeV
EIC-2	140 GeV	18 GeV	275 GeV

Table 1. The center-of-mass energies(\sqrt{S}) of representative electron-proton colliders, along with the corresponding energies of the electrons(E_e) and protons(E_P).

probe the partonic structure of the quasi-real photon. The quantity $d\hat{\sigma}(ij \rightarrow c\bar{b}[n] + b + \bar{c})$ is the short-distance partonic cross section, which can be calculated perturbatively within QCD. The intermediate heavy-quark pair $c\bar{b}[n]$ is characterized by the quantum numbers n , and the associated long-distance matrix element (LDME) $\langle \mathcal{O}^{B_c}[n] \rangle$ encodes the non-perturbative transition probability for the $c\bar{b}$ pair to hadronize into a physical B_c meson. In the present analysis, we restrict ourselves to the leading contribution in the NRQCD velocity expansion, namely the color-singlet channel $c\bar{b}[1]S_0^{[1]}$. Under this approximation, the corresponding LDME can be evaluated using potential models.

For definiteness, we consider the following partonic subprocesses contributing to three distinct production channels,

$$\gamma + g \rightarrow B_c(B_c^*, B_c(2^1S_0), B_c^*(2^3S_1)) + b + \bar{c}, \quad (2.3)$$

$$g + g \rightarrow B_c(B_c^*, B_c(2^1S_0), B_c^*(2^3S_1)) + b + \bar{c}, \quad (2.4)$$

$$q + \bar{q} \rightarrow B_c(B_c^*, B_c(2^1S_0), B_c^*(2^3S_1)) + b + \bar{c}, \quad (2.5)$$

where $q = u, d, s$. Representative Feynman diagrams for these subprocesses are shown in Figure 1. Both the analytical derivation and numerical evaluation of the partonic amplitudes are performed using the well-established FEYNMAN DIAGRAM CALCULATION (FDC) package [58]. Within this framework, the standard NRQCD projection method [59] is employed to extract contributions from specific heavy-quark configurations.

3 Numerical results and discussions

The input parameters in the calculation are taken as follows. The fine structure constant is fixed as $\alpha = 1/137$. $m_b = 4.8$ GeV, $m_c = 1.5$ GeV and $M_{B_c} = m_b + m_c$. The one-loop

colliders	$\sigma_{B_c}(\sigma_{\gamma g}, \sigma_{gg}, \sigma_{q\bar{q}})$	$\sigma_{B_c(2^1S_0)}(\sigma_{\gamma g}, \sigma_{gg}, \sigma_{q\bar{q}})$	$\sigma_{B_c^*}(\sigma_{\gamma g}, \sigma_{gg}, \sigma_{q\bar{q}})$	$\sigma_{B_c^*(2^3S_1)}(\sigma_{\gamma g}, \sigma_{gg}, \sigma_{q\bar{q}})$
HERA(pb)	0.44(0.43, 0.0085, 0.0023)	0.27(0.26, 0.0051, 0.0014)	2.19(2.15, 0.020, 0.016)	1.31(1.29, 0.012, 0.0096)
LHeC-1(pb)	3.69(3.51, 0.17, 0.0088)	2.21(2.10, 0.10, 0.0052)	16.99(16.51, 0.42, 0.056)	10.17(9.89, 0.25, 0.034)
LHeC-2(pb)	6.52(6.12, 0.38, 0.014)	3.90(3.67, 0.23, 0.0081)	29.50(28.48, 0.94, 0.087)	17.66(17.05, 0.56, 0.052)
FCC- <i>ep</i> -1(pb)	23.90(21.49, 2.38, 0.034)	14.31(12.86, 1.42, 0.020)	103.15(97.06, 5.88, 0.21)	61.75(58.11, 3.52, 0.126)
FCC- <i>ep</i> -2(pb)	34.36(30.41, 3.90, 0.045)	20.57(18.21, 2.33, 0.027)	147.00(137.07, 9.65, 0.28)	88.00(82.06, 5.78, 0.17)
EIC-1(fb)	0.70(0.67, 0.0013, 0.030)	0.42(0.400, 0.00081, 0.018)	3.96(3.71, 0.0027, 0.25)	2.37(2.22, 0.0016, 0.15)
EIC-2(fb)	72.06(70.61, 0.68, 0.77)	43.14(42.27, 0.41, 0.46)	378.16(370.97, 1.55, 5.64)	226.39(222.09, 0.93, 3.38)

Table 2. The integrated cross sections of the photoproduction of B_c at some typical electron-proton colliders. Each parenthesis contains three numerical values, which correspond respectively to the cross sections of the three production channels, Eq. (2.3,2.4,2.5).

running strong coupling constant is employed. The renormalization scale is set to be the transverse mass of the B_c meson, $\mu = \sqrt{M_{B_c}^2 + p_t^2}$ with p_t being its transverse momentum. The LDMEs $\langle \mathcal{O}^{B_c}[n] \rangle$ are related to the wave function at the origin, e.g., $\langle \mathcal{O}^{B_c}[n] \rangle \approx N_c |R_S(0)|^2 / (2\pi)$, with $|R_{1S}(0)|^2 = 1.642 \text{ GeV}^3$ and $|R_{2S}(0)|^2 = 0.983 \text{ GeV}^3$ [61, 62]. Several representative electron-proton colliders [63–66] were selected, and their corresponding center-of-mass energies are listed in Table 1.

The integrated cross sections for the photoproduction of B_c mesons at various electron-proton colliders are summarized in Table 2. The results are presented for both ground states (B_c , B_c^*) and excited states ($B_c(2^1S_0)$, $B_c^*(2^3S_1)$), with contributions from three distinct production channels: the direct photoproduction process $\gamma + g \rightarrow B_c + b + \bar{c}$, and the resolved photoproduction processes $g + g \rightarrow B_c + b + \bar{c}$ and $q + \bar{q} \rightarrow B_c + b + \bar{c}$ (where $q = u, d, s$). Table 2 reveals a clear energy dependence in the relative importance of these channels:

- At HERA ($\sqrt{S} = 319 \text{ GeV}$), the resolved gg channel accounts for only $\sim 1.9\%$ of the total B_c cross section, while the $q\bar{q}$ channel is negligible ($\sim 0.5\%$). The direct γg process dominates ($\sim 97.6\%$), consistent with expectations at lower collision energies.
- At LHeC-2 ($\sqrt{S} = 1.98 \text{ TeV}$), the gg contribution rises to $\sim 5.8\%$, while the $q\bar{q}$ channel remains small ($\sim 0.2\%$). The γg channel still dominates ($\sim 93.9\%$), but the enhanced gluon density at higher energies begins to manifest.
- Most significantly, at FCC-*ep*-2 ($\sqrt{S} = 10.0 \text{ TeV}$), the gg contribution reaches $\sim 11.4\%$, highlighting its importance in high-energy regimes. This substantial contribution underscores the necessity of including resolved processes for precision predictions at future colliders like the FCC-*ep*.

The $q\bar{q}$ channel remains consistently negligible across all colliders ($< 1\%$), as expected due to the suppression of quark-initiated processes in photoproduction. The cross sections for excited states follow similar patterns, with the B_c^* states having larger cross sections due to their spin-triplet configuration. Future electron–proton colliders are designed to operate at very high luminosities. Taking the FCC-*ep* as a representative example, its projected integrated luminosity can reach the order of 1 ab^{-1} . Combined with the total cross sections listed in Table 2, this implies that approximately $\mathcal{O}(10^8)$ B_c mesons could be produced at the FCC-*ep*. In contrast, the planned luminosity of the EIC is relatively lower. After further

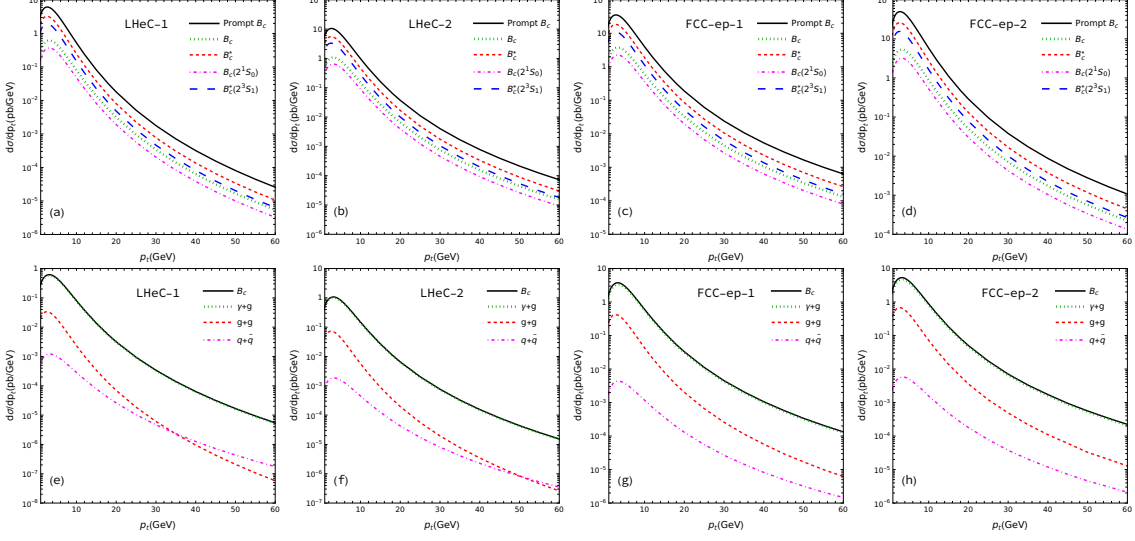


Figure 2. The p_t distributions for B_c photoproduction. (a,b,c,d): p_t distributions of four B_c states and “prompt B_c ” means production of the ground B_c after including the feed-down contributions from excited states with 100% decay probability to it. (e,f,g,h): p_t distributions for the channels in Eq. (2.3,2.4,2.5) of the ground B_c production.

accounting for realistic experimental detection and reconstruction efficiencies, only a limited number of B_c events are expected to be observable at the EIC. Although the $\gamma + g$ channel provides the dominant contribution to the total cross section, the $g + g$ resolved channel can reach the level of $\mathcal{O}(10\%)$, indicating that it constitutes a non-negligible component of B_c photoproduction at ep colliders.

The transverse momentum (p_t) distributions for B_c photoproduction provide deeper insights into the kinematic features of different production mechanisms. Figure 2 presents these distributions for LHeC and FCC- ep configurations. From Figure 2(a–d), which display the relative contributions to the prompt B_c yield from different intermediate states, one observes a clear dependence on the transverse momentum. The distributions for all B_c states (B_c , B_c^* , $B_c(2^1S_0)$, $B_c(2^3S_1)$) exhibit similar shapes, peaking at low p_t and decreasing rapidly with increasing transverse momentum. The contribution from the pseudoscalar state $B_c(1^1S_0)$ increases with increasing p_T , whereas the contribution from the vector state $B_c^*(3^3S_1)$ shows a mild decrease as p_T grows.

As shown in Figure 2(e–h), the contribution from the $\gamma + g$ channel dominates the photoproduction cross section over the entire p_T region. This behavior is consistent with the integrated cross-section results presented in Table 2. A closer inspection of the figures reveals that the contribution from the $g + g$ channel decreases with increasing p_T , while the $q + \bar{q}$ contribution exhibits the opposite trend and becomes relatively more important at large transverse momentum. As a representative example, at FCC- ep -2 the $g + g$ channel contributes about 15.82% of the total cross section at $p_T = 1$ GeV, whereas this fraction is reduced to 5.82% at $p_T = 50$ GeV. In realistic experimental conditions, however, the majority of events are produced in the low- p_T region. This further highlights the importance

m_c (GeV)	1.4	1.5	1.6
σ_{B_c}	8.15(42.64)	6.52(34.36)	5.29(28.08)
$\sigma_{B_c(2^1S_0)}$	4.88(25.53)	3.90(20.57)	3.16(16.81)
$\sigma_{B_c^*}$	36.96(183.31)	29.50(147.00)	23.86(120.05)
$\sigma_{B_c^*(2^3S_1)}$	22.13(109.74)	17.66(88.00)	14.28(71.87)

Table 3. Variations of the integrated cross sections (in unit of pb) by m_c for the photoproduction of B_c under LHeC-2 and FCC- ep -2 energy (values in brackets) respectively. Three channels of Eq. (2.3,2.4,2.5) have been summed up.

m_b (GeV)	4.7	4.8	4.9
σ_{B_c}	7.15(37.40)	6.52(34.36)	5.96(31.62)
$\sigma_{B_c(2^1S_0)}$	4.28(22.39)	3.90(20.57)	3.57(18.93)
$\sigma_{B_c^*}$	32.30(159.60)	29.50(147.00)	27.00(135.20)
$\sigma_{B_c^*(2^3S_1)}$	19.34(95.54)	17.66(88.00)	16.16(80.94)

Table 4. Variations of the integrated cross sections (in unit of pb) by m_b for the photoproduction of B_c under LHeC-2 and FCC- ep -2 energy (values in brackets) respectively. Three channels of Eq. (2.3,2.4,2.5) have been summed up.

\mathcal{C}	0.5	1.0	2.0
σ_{B_c}	9.73(19.68)	6.52(34.36)	4.58(27.12)
$\sigma_{B_c(2^1S_0)}$	5.82(11.78)	3.90(20.57)	2.74(16.24)
$\sigma_{B_c^*}$	43.91(86.59)	29.50(147.00)	20.78(116.33)
$\sigma_{B_c^*(2^3S_1)}$	26.29(51.84)	17.66(88.00)	12.44(69.64)

Table 5. Variations of the integrated cross sections (in unit of pb) by $\mu = \mathcal{C} \sqrt{M_{B_c}^2 + p_t^2}$ with $\mathcal{C} = 0.5, 1, 2$, for the photoproduction of B_c under LHeC-2 and FCC- ep -2 energy (values in brackets) respectively. Three channels of Eq. (2.3,2.4,2.5) have been summed up.

of including the $g + g$ resolved photoproduction channel in theoretical calculations.

We now turn to the theoretical uncertainties of our predictions. Tables 3 and 4 show the dependence of the total cross sections on the heavy-quark masses m_c and m_b , respectively. The cross section exhibits a stronger sensitivity to the charm-quark mass than to the bottom-quark mass. A variation of m_c by ± 0.1 GeV around its central value leads to a change of about 20%–30% in the cross section, reflecting the fact that the $c\bar{b}$ pair is produced close to threshold. By contrast, varying m_b within the same range induces a more moderate effect, typically at the level of 5%–10%.

The uncertainty associated with the choice of renormalization scales is presented in Table 5. As expected for a leading-order calculation, the scale dependence constitutes the dominant source of theoretical uncertainty. Varying the scale from $0.5\mu_0$ to $2\mu_0$, with $\mu_0 = \sqrt{M_{B_c}^2 + p_T^2}$, results in variations of the total cross section of order 30% or larger. This behavior indicates the potential importance of higher-order QCD corrections, which are beyond the scope of the present work.

4 Summary

In this work, we have performed a comprehensive analysis of B_c meson photoproduction at electron–proton colliders within the NRQCD factorization approach. The photoproduction of both ground states (B_c , B_c^*) and excited states ($B_c(2^1S_0)$, $B_c^*(2^3S_1)$) have been investigated. It shows that cross sections of excited states are comparable to, or even larger than, that of the ground state. Assuming subsequent decays into the ground-state B_c , the feed-down contributions significantly enhance the prompt B_c yield and should be included in realistic phenomenological studies. Both direct and resolved photoproduction mechanisms have been considered, including the subprocesses $\gamma + g$, $g + g$, and $q + \bar{q}$. The direct $\gamma + g$ channel dominates the B_c photoproduction cross section over the entire kinematic range. Nevertheless, the resolved $g + g$ contribution is not negligible and can reach the $\mathcal{O}(10\%)$ level in the low- p_T region, which accounts for the majority of produced events. The $q + \bar{q}$ channel, although exhibiting a relatively harder p_T spectrum, remains numerically suppressed and can be safely neglected in practical calculations.

Acknowledgments

The work has been supported partly by the National Natural Science Foundation of China (NNSFC) with Grants No. 12305083 and No. 12235008.

References

- [1] C.-H. Chang and Y.-Q. Chen, [The hadronic production of the \$B\(c\)\$ meson at Tevatron, CERN LHC and SSC](#), [Phys. Rev. D](#) **48** (1993) 4086.
- [2] C.-H. Chang, Y.-Q. Chen, G.-P. Han and H.-T. Jiang, [On hadronic production of the \$B\(c\)\$ meson](#), [Phys. Lett. B](#) **364** (1995) 78 [[hep-ph/9408242](#)].
- [3] CDF collaboration, [Observation of the \$B_c\$ meson in \$p\bar{p}\$ collisions at \$\sqrt{s} = 1.8\$ TeV](#), [Phys. Rev. Lett.](#) **81** (1998) 2432 [[hep-ex/9805034](#)].
- [4] CDF collaboration, [Observation of \$B_c\$ mesons in \$p\bar{p}\$ collisions at \$\sqrt{s} = 1.8\$ TeV](#), [Phys. Rev. D](#) **58** (1998) 112004 [[hep-ex/9804014](#)].
- [5] ATLAS collaboration, [Observation of an Excited \$B_c^\pm\$ Meson State with the ATLAS Detector](#), [Phys. Rev. Lett.](#) **113** (2014) 212004 [[1407.1032](#)].
- [6] CMS collaboration, [Observation of Two Excited \$B_c^+\$ States and Measurement of the \$B_c^+\(2S\)\$ Mass in \$pp\$ Collisions at \$\sqrt{s} = 13\$ TeV](#), [Phys. Rev. Lett.](#) **122** (2019) 132001 [[1902.00571](#)].
- [7] LHCb collaboration, [Observation of an excited \$B_c^+\$ state](#), [Phys. Rev. Lett.](#) **122** (2019) 232001 [[1904.00081](#)].
- [8] LHCb collaboration, [Observation of Orbitally Excited \$B_c^+\$ States](#), [Phys. Rev. Lett.](#) **135** (2025) 231902 [[2507.02149](#)].
- [9] K. Kolodziej, A. Leike and R. Ruckl, [Production of \$B\(c\)\$ mesons in hadronic collisions](#), [Phys. Lett. B](#) **355** (1995) 337 [[hep-ph/9505298](#)].

[10] E. Braaten, K.-m. Cheung and T.C. Yuan,
Perturbative QCD fragmentation functions for B_c and B_c^* production, [Phys. Rev. D **48** \(1993\) R5049](#) [[hep-ph/9305206](#)].

[11] A.V. Berezhnoy, A.K. Likhoded and M.V. Shevlyagin, Hadronic production of B(c) mesons, [Phys. Atom. Nucl. **58** \(1995\) 672](#) [[hep-ph/9408284](#)].

[12] S.S. Gershtein, V.V. Kiselev, A.K. Likhoded and A.V. Tkabladze, Physics of B(c) mesons, [Phys. Usp. **38** \(1995\) 1](#) [[hep-ph/9504319](#)].

[13] C.-H. Chang, Y.-Q. Chen and R.J. Oakes,
Comparative study of the hadronic production of B(c) mesons, [Phys. Rev. D **54** \(1996\) 4344](#) [[hep-ph/9602411](#)].

[14] A.V. Berezhnoy, V.V. Kiselev and A.K. Likhoded,
Hadronic production of S and P wave states of anti-b c quarkonium, [Z. Phys. A **356** \(1996\) 79](#) [[hep-ph/9602347](#)].

[15] S.P. Baranov, Pair production of B(c)* mesons in p p and gamma gamma collisions, [Phys. Rev. D **55** \(1997\) 2756](#).

[16] S.P. Baranov,
Semiperturbative and nonperturbative production of hadrons with two heavy flavors, [Phys. Rev. D **56** \(1997\) 3046](#).

[17] K.-m. Cheung, B_c meson production at the Tevatron revisited, [Phys. Lett. B **472** \(2000\) 408](#) [[hep-ph/9908405](#)].

[18] C.-H. Chang and X.-G. Wu,
Uncertainties in estimating hadronic production of the meson B_c and comparisons between TEVATRON and LHC, [Eur. Phys. J. C **38** \(2004\) 267](#) [[hep-ph/0309121](#)].

[19] C.-H. Chang, J.-X. Wang and X.-G. Wu,
Hadronic production of the P-wave excited B_c -states $B^*(cJ, L=1)$, [Phys. Rev. D **70** \(2004\) 114019](#) [[hep-ph/0409280](#)].

[20] C.-H. Chang, C.-F. Qiao, J.-X. Wang and X.-G. Wu,
The Color-octet contributions to P-wave B_c meson hadroproduction, [Phys. Rev. D **71** \(2005\) 074012](#) [[hep-ph/0502155](#)].

[21] C.-H. Chang, C.-F. Qiao, J.-X. Wang and X.-G. Wu,
Hadronic production of $B_c(B_c^*)$ meson induced by the heavy quarks inside the collision hadrons, [Phys. Rev. D **72** \(2005\) 114009](#) [[hep-ph/0509040](#)].

[22] C.-H. Chang, C. Driouichi, P. Eerola and X.G. Wu,
BCVEGPY: An Event generator for hadronic production of the B_c meson, [Comput. Phys. Commun. **159** \(2004\) 192](#) [[hep-ph/0309120](#)].

[23] C.-H. Chang, J.-X. Wang and X.-G. Wu,
BCVEGPY2.0: A Upgrade version of the generator BCVEGPY with an addendum about hadroproduction of the B_c meson, [Comput. Phys. Commun. **174** \(2006\) 241](#) [[hep-ph/0504017](#)].

[24] X.-Y. Wang and X.-G. Wu,
A Trick to Improve the Efficiency of Generating Unweighted B_c Events from BCVEGPY, [Comput. Phys. Commun. **183** \(2012\) 442](#) [[1108.2442](#)].

[25] H.-Y. Bi, R.-Y. Zhang, H.-Y. Han, Y. Jiang and X.-G. Wu,

Photoproduction of the $B_c^{(*)}$ meson at the LHeC, [Phys. Rev. D](#) **95** (2017) 034019 [[1612.07990](#)].

[26] G. Chen, C.-H. Chang and X.-G. Wu,
 $B_c(B_c^*)$ meson production via the proton-nucleus and the nucleus-nucleus collision modes at the colliders RHIC [Phys. Rev. D](#) **97** (2018) 114022 [[1803.11447](#)].

[27] A.V. Berezhnoy, I.N. Belov, A.K. Likhoded and A.V. Luhinsky,
 B_c excitations at LHC experiments, [Mod. Phys. Lett. A](#) **34** (2019) 1950331 [[1904.06732](#)].

[28] Z. Yang, X.-G. Wu, G. Chen, Q.-L. Liao and J.-W. Zhang,
 B_c Meson Production around the Z^0 Peak at a High Luminosity e^+e^- Collider, [Phys. Rev. D](#) **85** (2012) 094015 [[1112.5169](#)].

[29] G. Chen, X.-G. Wu, Z. Sun, X.-C. Zheng and J.-M. Shen,
Next-to-leading order QCD corrections for the charmonium production via the channel $e^+e^- \rightarrow H(|c\bar{c}\rangle) + \gamma$ round [Phys. Rev. D](#) **89** (2014) 014006 [[1311.2735](#)].

[30] G. Chen, X.-G. Wu, Z. Sun, S.-Q. Wang and J.-M. Shen,
Exclusive charmonium production from e^+e^- annihilation round the Z^0 peak, [Phys. Rev. D](#) **88** (2013) 074021 [[1308.5375](#)].

[31] Z. Sun, X.-G. Wu, G. Chen, J. Jiang and Z. Yang,
Heavy quarkonium production through the semi-exclusive e^+e^- annihilation channels round the Z^0 peak, [Phys. Rev. D](#) **87** (2013) 114008 [[1302.4282](#)].

[32] G. Chen, X.-G. Wu, H.-B. Fu, H.-Y. Han and Z. Sun,
Photoproduction of heavy quarkonium at the ILC, [Phys. Rev. D](#) **90** (2014) 034004 [[1407.3650](#)].

[33] Z. Sun, X.-G. Wu, G. Chen, Y. Ma, H.-H. Ma and H.-Y. Bi,
Bottomonium production associated with a photon at a high luminosity e^+e^- collider with the one-loop QCD correction, [Phys. Rev. D](#) **89** (2014) 074035 [[1401.2735](#)].

[34] Z. Sun, X.-G. Wu and H.-F. Zhang,
Prompt J/ψ production in association with a $c\bar{c}$ pair within the framework of nonrelativistic QCD via photon-pair production, [Phys. Rev. D](#) **92** (2015) 074021 [[1507.08190](#)].

[35] Y.-B. Wei, R.-H. Li, D. Luo, C.-D. Lü and Y.-L. Shen,
Exclusive production of B_c mesons in e^+e^- colliders, [Chin. Phys. C](#) **42** (2018) 083107 [[1807.05776](#)].

[36] Z.-G. He and B.A. Kniehl, Perspectives of heavy-quarkonium production at FCC-ee, [CERN Yellow Reports: Monographs](#) **3** (2020) 89.

[37] Z. Yang, X.-G. Wu and X.-Y. Wang,
BEEC: An event generator for simulating the B_c meson production at an e^+e^- collider, [Comput. Phys. Commun.](#) **184** (2013) 2848 [[1305.4828](#)].

[38] Z. Yang, X.-C. Zheng and X.-G. Wu,
BEEC2.0: An upgraded version for the production of heavy quarkonium at electron-positron collider, [Comput. Phys. Commun.](#) **281** (2022) 108503 [[2208.00876](#)].

[39] X.-P. Wang, Y.-J. Li, G.-Z. Xu and K.-Y. Liu,
Relativistic corrections to double B_c meson production in e^+e^- annihilation, [2512.20526](#).

[40] C.-H. Chang and Y.-Q. Chen,

The Production of B(c) or anti-B(c) meson associated with two heavy quark jets in Z0 boson decay, [Phys. Rev. D 46 \(1992\) 3845](#).

- [41] C.-H. Chang, J.-X. Wang and X.-G. Wu,
Production of B_c or \bar{B}_c meson and its excited states via \bar{t} quark or t quark decays, [Phys. Rev. D 77 \(2008\) 014022 \[0711.1898\]](#).
- [42] L.-C. Deng, X.-G. Wu, Z. Yang, Z.-Y. Fang and Q.-L. Liao,
 Z_0 Boson Decays to $B_c^{(*)}$ Meson and Its Uncertainties, [Eur. Phys. J. C 70 \(2010\) 113 \[1009.1453\]](#).
- [43] Z. Yang, X.-G. Wu, L.-C. Deng, J.-W. Zhang and G. Chen,
Production of the P -Wave Excited B_c -States through the Z^0 Boson Decays, [Eur. Phys. J. C 71 \(2011\) 1563 \[1011.5961\]](#).
- [44] J. Jiang, L.-B. Chen and C.-F. Qiao,
QCD NLO corrections to inclusive B_c^* production in Z^0 decays, [Phys. Rev. D 91 \(2015\) 034033 \[1501.00338\]](#).
- [45] J. Jiang and C.-F. Qiao, B_c Production in Higgs Boson Decays, [Phys. Rev. D 93 \(2016\) 054031 \[1512.01327\]](#).
- [46] X.-C. Zheng, C.-H. Chang, X.-G. Wu, J. Zeng and X.-D. Huang,
Next-to-leading order QCD corrections to the production of B_c and B_c^* through W^+ -boson decays, [Phys. Rev. D 101 \(2020\) 034029 \[1911.12531\]](#).
- [47] D. Yang and W. Zhang,
Relativistic corrections of the fragmentation functions for a heavy quark to B_c and B_c^* , [Chin. Phys. C 43 \(2019\) 083101 \[1905.02923\]](#).
- [48] Z.-Q. Chen, H. Yang and C.-F. Qiao,
NLO QCD corrections to B_c -pair production in photon-photon collision, [Phys. Rev. D 102 \(2020\) 016011 \[2005.07317\]](#).
- [49] X.-C. Zheng, X.-G. Wu, X.-J. Zhan, G.-Y. Wang and H.-T. Li,
Higgs boson decays to B_c meson in the fragmentation-function approach, [Phys. Rev. D 107 \(2023\) 074005 \[2301.06383\]](#).
- [50] H.-Y. Bi, R.-Y. Zhang, X.-G. Wu, W.-G. Ma, X.-Z. Li and S. Owusu,
Photoproduction of doubly heavy baryon at the LHeC, [Phys. Rev. D 95 \(2017\) 074020 \[1702.07181\]](#).
- [51] K. He, H.-Y. Bi, R.-Y. Zhang, X.-Z. Li and W.-G. Ma,
P-wave excited B_c^{**} meson photoproduction at the LHeC, [J. Phys. G 45 \(2018\) 055005 \[1710.11508\]](#).
- [52] Z. Sun and X.-G. Wu,
The production of the doubly charmed baryon in deeply inelastic ep scattering at the Large Hadron Electron Collider, [JHEP 07 \(2020\) 034 \[2004.01012\]](#).
- [53] H. Yang, Z.-Q. Chen and C.-F. Qiao,
NLO QCD corrections to pseudoscalar quarkonium production with two heavy flavors in photon-photon collision, [Phys. Rev. D 105 \(2022\) 094014 \[2203.14204\]](#).
- [54] X.-J. Zhan, X.-G. Wu and X.-C. Zheng,
Photoproduction of the B_c meson at future e^+e^- colliders, [Phys. Rev. D 106 \(2022\) 094036 \[2211.09003\]](#).

[55] G.T. Bodwin, E. Braaten and G.P. Lepage, Rigorous QCD analysis of inclusive annihilation and production of heavy quarkonium, [Phys. Rev. D51 \(1995\) 1125 \[hep-ph/9407339\]](#).

[56] S. Frixione, M.L. Mangano, P. Nason and G. Ridolfi, Improving the Weizsäcker-Williams approximation in electron - proton collisions, [Phys. Lett. B319 \(1993\) 339 \[hep-ph/9310350\]](#).

[57] M. Gluck, E. Reya and I. Schienbein, Radiatively generated parton distributions of real and virtual photons, [Phys. Rev. D60 \(1999\) 054019 \[hep-ph/9903337\]](#).

[58] J.-X. Wang, Progress in FDC project, [Nucl. Instrum. Meth. A534 \(2004\) 241 \[hep-ph/0407058\]](#).

[59] G.T. Bodwin and A. Petrelli, Order- v^4 corrections to S -wave quarkonium decay, [Phys. Rev. D 66 \(2002\) 094011 \[hep-ph/0205210\]](#).

[60] D. Binosi and L. Theussl, JaxoDraw: A Graphical user interface for drawing Feynman diagrams, [Comput. Phys. Commun. 161 \(2004\) 76 \[hep-ph/0309015\]](#).

[61] E.J. Eichten and C. Quigg, Mesons with beauty and charm: Spectroscopy, [Phys. Rev. D 49 \(1994\) 5845 \[hep-ph/9402210\]](#).

[62] E.J. Eichten and C. Quigg, Quarkonium wave functions at the origin, [Phys. Rev. D52 \(1995\) 1726 \[hep-ph/9503356\]](#).

[63] H1, ZEUS collaboration, New Results on Charm Production at HERA, [Acta Phys. Polon. Supp. 7 \(2014\) 511](#).

[64] LHEC STUDY GROUP collaboration, A Large Hadron Electron Collider at CERN: Report on the Physics and Design Concepts for Machine and Detector, [J. Phys. G 39 \(2012\) 075001 \[1206.2913\]](#).

[65] Y.C. Acar, A.N. Akay, S. Beser, A.C. Canbay, H. Karadeniz, U. Kaya et al., Future circular collider based lepton–hadron and photon–hadron colliders: Luminosity and physics, [Nucl. Instrum. Meth. A 871 \(2017\) 47 \[1608.02190\]](#).

[66] A. Accardi et al., Electron Ion Collider: The Next QCD Frontier: Understanding the glue that binds us all, [Eur. Phys. J. A 52 \(2016\) 268 \[1212.1701\]](#).